We are IntechOpen, the world's leading publisher of Open Access books Built by scientists, for scientists

4,800
Open access books available

122,000
International authors and editors

135M
Downloads

Our authors are among the

154
Countries delivered to

TOP 1%
most cited scientists

12.2%
Contributors from top 500 universities

WEB OF SCIENCE™

Selection of our books indexed in the Book Citation Index in Web of Science™ Core Collection (BKCI)

Interested in publishing with us?
Contact book.department@intechopen.com

Numbers displayed above are based on latest data collected.
For more information visit www.intechopen.com

Chapter 8

A Novel Application of Oceanic Biopolymers — Strategic Regulation of Polymer Characteristics for Membrane Technology in Separation Engineering

Keita Kashima, Ryuhei Nomoto and Masanao Imai

Additional information is available at the end of the chapter

http://dx.doi.org/10.5772/61998

Abstract

Membranes prepared from oceanic biopolymers have a high potential in membrane separation processes and water purification. It is anticipated to result in more biocompatible and lower-cost materials compared with artificial polymers. This chapter describes the excellent performance of oceanic biopolymer membranes in separation engineering and the regulation factors controlling membrane properties. In particular, chitosan and alginate were picked up as intelligent membrane materials to provide the promised molecular size recognition and other membrane properties. Future prospective strategies for a simple methodology for preparing stable membranes from oceanic biopolymers and the development of selective separation processing were reviewed.

Keywords: Membrane, oceanic biopolymer, chitosan, alginate, mechanical strength, mass transfer characteristics

1. Introduction

1.1. Overview of oceanic biopolymers in membrane separation technology

Membrane separation technology has been applied in various fields, such as the chemical industry, food production, pharmaceutical products, environmental sciences, and water purification, because it can be operated without heating and residual toxicity. Its energy cost was lower than conventional thermal separation technologies [1–4]. It can be employed for broad components by selecting optimum membranes.

Development of oceanic biopolymer membranes such as chitosan and alginate has exponentially increased due to increases in the demand for biocompatibility, environment adaptability,

renewability, and selective separation ability [5–6]. In the field of membrane science, most membranes have been made from petroleum-based polymers used as raw materials for the membrane body. Petroleum-based synthetic polymers such as polyethylene, polyamide, polyimide, and polysulfonate have been used as the main materials of the membrane body for a long time. The practical use of biopolymer membranes was less than synthetic polymer membranes, because controlling the physical and chemical properties of a biopolymer produced from natural bioresources was difficult in practical membrane applications. Cellulose-based membranes have been extensively used in practical applications since the development of the anisotropic cellulose acetate membrane in 1963 by Loeb and Sourirajan [7]. Applications of biopolymer materials have increased recently for membrane sciences [8]. Recent studies of biopolymer membranes are summarized in Table 1 referred to previous literatures [9-22]. In the past five years, oceanic biopolymers have attracted attention for their chemical functional ability. Investigations of oceanic biopolymer membranes, especially chitosan and alginate, for various applications have drastically increased.

Authors	Year	Membrane materials	Application	Coments	Ref.
Torres et al.	2010	eggshell	biomedical application	regenerative medicine	9
Kashima et al.	2010	calcium alginate	membrane separation	mass transfer characteristics	10
Kashima and Imai	2011	calcium alginate	membrane separation	mass transfer characteristics	11
Michalak and Mucha	2012	polylactid acid, dibutyrylchitin, chitosan	controlled release	drug delivery system	12
Wu and Imai	2013	pullulan and κ-carrageenan	membrane separation	dyes removal	13
Lakra et al.	2013	chitosan or cellulose brended polyethersulfone	membrane separation	food industry	14
Moraes et al.	2013	chitosan and alginate	membrane separation	environment science	15
Nomoto and Imai	2014	chitosan	membrane separation	mass transfer characteristics	16
Ma et al.	2014	chitosan	biomedical application	guided bone regeneration	17
Uragami et al.	2015	chitosan	membrane separation	pervaporative dehydration	18
Alias et al.	2015	chitosan blended SiO_2	membrane separation	proton battery	19
Puspasari et al.	2015	cellulose	membrane separation	nanofiltration	20
Livazovic et al.	2015	cellulose	membrane separation	water treatment	21
Zhang et al.	2015	calcium alginate and polyacrylamide	membrane separation	nanofiltration	22

Kashima, Nomoto and Imai 2015.

Table 1. Recent investigations of biopolymer membrane and applications.

The common aim of membrane separation technology is to separate a target component from a mixture with the aid of permeation through the membrane, while rejecting other components. The key characteristics for practical use are as follows: mechanical strength, permeation flux, diffusivity of molecule, and micro-/nanostructure. This chapter describes the dominant factors in controlling important properties for practical membrane separation applications for oceanic polymer membrane, especially those of chitosan and alginate.

2. Chitosan membrane

Chitosan is a well-known sustainable and biocompatible oceanic biomaterial. It has been attracted in creating new polymer materials for broad application due to its nontoxicity,

http://dx.doi.org/10.5772/61998

biocompatibility, and biodegradability [5]. Chitosan is refined by removing an acetyl group from chitin, which is mainly produced in oceanic bioresources such as the shells of crabs and shrimps. Chitin is the second most abundant natural polymer in nature, after cellulose [23]. Chitosan is generally discarded as industrial waste around the world [24]. It is strongly expected to be useful as a biocompatible and reactive material for making functional gel membranes. Recent studies of various chitosan membranes are summarized in Table 2 and Table 3 referred to previous literatures [5-6, 12, 15-19, 24-46].

2.1. Chemical composition and membrane formation

Chitosan is a heteropolymer obtained by alkaline deacetylation of chitin at the C-2 position as shown in Figure 1 (a) and (b). Chitosan is generally defined by a deacetylation degree (*DD* [%]) of 60–100%. The deacetylation degree is estimated as follows:

$$DD = \frac{n_{GS}}{n_{GS} + n_{AGS}} \times 100 \tag{1}$$

Here, n_{GS} (n_{AGS}) is the molar number of glucosamine residues (acetylglucosamine residues) in the molecular chain. Chitosan has great potential for chemical modification because its molecular chain has a rich amino group and a hydroxyl group in the glucosamine residues [29].

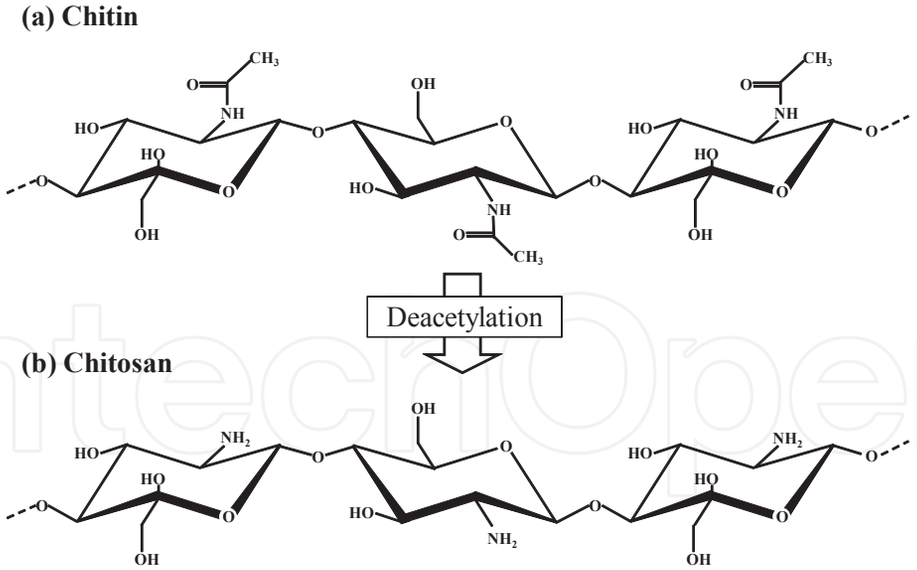

Figure 1. Chemical structure of chitosan showing β-1,4-D-glycoside linkage. (a) Chitin molecular chain consisting of poly-β-1,4-D-*N*-acetylglucosamine residues, (b) chitosan molecular chain consisting of poly-β-1,4-D-glucosamine residues.

The beneficial effects of chitosan are as a dietary fiber, such as its inhibition of fat digestibility [47] and its reduction of cholesterols [48]. The biodegradability and biocompatibility of chitosan are also suitable for biomedical applications [49].

Kashima, Nomoto and Imai 2015.

Table 2. Recent investigations of chitosan membrane (2012–2014).

Authors	Year	Membrane material	Application	Raguration factor	Controled properties of membrane	Coments	Ref.
Michalak and Mucha	2012	chitosan blended polylactid acid and dibutyrylchitin	controlled release	-	-	drug delivery system	12
Tasselli et al.	2013	chitosan	membrane separation	concentration of glutataldehyde as a cross-linker	mechanical strength, swelling ratio, adsorption of dye	hollow fiber membrane	25
Moraes et al.	2013	alginate blended chitosan	membrane separation	blended chitosan	swelling ratio, thickness, adsorption of herbicide	water treatment	15
Sun et al.	2014	chitosan	antibacterial medium	concentration of gallic acid	antibacterial activity, mechanical strength	food packaging film	26
Wanichapichart et al.	2014	chitosan blended polysulfone	membrane separation	mixing ratio of chitosan and polysulfone	water permeation coefficient, rejection of fluoride and cadmium	water treatment	27
Ma et al.	2014	chitosan containing chitin whisker	biomedical application	containing ratio of chitin whisker	mechanical strength, antibacterial activity	wound dressing	5
Bai et al.	2014	chitosan containing nanotube bearing sulfonate polyelectrolyte	fuel cell	containing ratio of nanotube	water uptake, proton conductivity, methanol permeability	direct methanol fuel cell	24
Nomoto and Imai	2014	chitosan	membrane separation	concentration of NaOH for neutralization of chitosan	mechanical strength, porosity, water permeation flux, effective diffusion coefficient	mass transfer characteristics	16
Shenvi et al.	2014	chitosan supported on PPEES membrane	membrane separation	pH of tripolyphosphate solution as a cross-linker	water flux, water uptake, salts rejection	water treatment	28
Han et al.	2014	alginate and chitosan	biomedical application	-	-	wound dressing	29
Karim et al.	2014	chitosan containing cellulose nanocrystals	membrane separation	with or without cross-linking by gluteraldehyde	dyes rejection, porosity, mechanical strength	dyes purification	30
Dudek et al.	2014	chitosan containing ion oxide nanoparticles	membrane separation	containing ratio of iron oxide, additive sulphuric acid or glutaraldehyde	water permeation coefficient of water and ethanol	pervaporative dehydration	31
Kumar et al.	2014	polysulfone blended chitosan and functionalized chitosan	membrane separation	functionalization of chitosan molecular chain	heavy metal rejection, atifouling activity	heavy metal purification	32
Bueno et al.	2014	chitosan and alginate based	biomedical application	containing ratio of surfactant (Pluronic F68)	porosity, mechanical strength	wound dressing	6
Ma et al.	2014	chitosan	biomedical application	cross-linking with tripolyphosphate	mechanical strength, biocompatibility	guided bone regeneration	17

PES: polyethersulfone, PDMCHEA:poly (2-methacryloyloxy ethyl trimethylammonium chloride-co-2-hydroxyethyl acrylate), PPEES: poly (1, 4-phenylene ether ether sulfone), PVP: polyvinylpyrrolidone

http://dx.doi.org/10.5772/61998

Chitosan is dissolved in an acid aqueous solution, such as acetic acid. To form a water-insoluble chitosan membrane, the acetic acid has to be neutralized by basic components. The authors have reported preparation of chitosan membrane using casting methods [16]. For example, 4 g of chitosan was dissolved in 198 mL of 1.7 mol·L^{-1} acetic acid aqueous solution. The solution was mixed magnetically for 12 h at room temperature to obtain a mature solution. Some insoluble matter was removed by vacuum filtration using a filter paper (Grade No. 1, ADVANTEC, Japan). The concentration of the chitosan casting solution was 0.02 $g_{\text{-chitosan}}$·$mL_{\text{-chitosan casting solution}}^{-1}$. Ten grams of the casting solution was dispensed in a glass Petri dish (inner diameter 7.75 cm) and dried in a thermostatic chamber at 333 K for 24 h. A dried chitosan membrane formed on the glass Petri dish. A 20 mL of sodium hydroxide (NaOH) aqueous solution was directly introduced onto the dried chitosan membrane. The chitosan membrane was continuously immersed for 3 h in NaOH solution for neutralization. The concentration of the supplied NaOH ranged from 0.1 to 5 mol·L^{-1}. In this case, the stoichiometric equivalent concentration of NaOH was estimated to be 0.83 mol·L^{-1}. After neutralization, the swollen membrane was easily separated from the glass Petri dish and was washed fully with pure water to remove excess NaOH.

2.2. Dominant role of the acid–base neutralization in chitosan membrane characteristics

The authors previously reported the dominant role of the acid–base neutralization process in forming chitosan membranes for controlling some membrane properties [16].

2.2.1. Mechanical strength

The mechanical strength, maximum tensile stress (Figure 2a), and maximum strain (Figure 2b) at membrane rupture presented bell-shaped curves with peaks when the NaOH concentration increased. For an 81% *DD* chitosan membrane, the maximum stress and the maximum strain reached maximum values of 8.6 MPa and 80.5%, respectively, in a membrane prepared with 1 mol·L^{-1} NaOH. This concentration was almost the same as the stoichiometric equivalent concentration (0.83 mol·L^{-1}). In contrast, in a 98% *DD* chitosan membrane, the maximum stress and the maximum strain increase to 17.9 MPa and 134% when the membrane was prepared with 2 mol·L^{-1} NaOH.

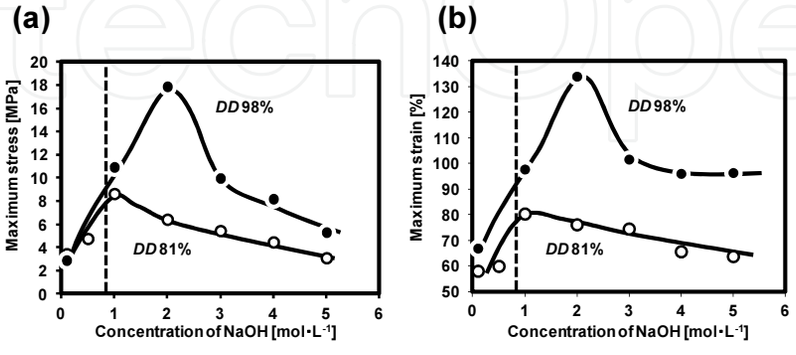

Figure 2. Effect of NaOH concentration in neutralization on the maximum stress (a) and maximum strain (b) at membrane rupture in reference [16]. The dashed line represents the stoichiometric neutralization concentration of NaOH (0.83 mol·L^{-1}).

Kashima, Nomoto and Imai 2015.

Table 3. Most recent investigations of chitosan membrane (2015).

Authors	Year	Membrane materials	Application	Raguration factors	Controled properties	Coments	Ref.
Sajjan et al.	2015	GTMAC grafted chitosan	membrane separation	mixing ration of chitosan	hydrophilicity, water/isopropanaol selectivity	pervaporative dehydration	33
Bibi et al.	2015	chitosan containing carbon nanotube	membrane separation	with or without carbon nanotube	pore size, swelling ratio, adsorption of naphthalene	water treatment	34
Ji et al.	2015	chitosan blended PDMCHEA	membrane separation	mixing ratio of PDMCHEA	water flux, mechanical strength, hydrophilicity	nanofiltration membrane	35
Uragami et al.	2015	chitosan	membrane separation	molecular weight and degree of deacetylation	permeation flux, water/ethanol selectivity	pervaporative dehydration	18
Premakshi et al.	2015	chitosan	membrane separation	additive concentration of zeolite	mechanical strength, permeation flux, water/isopropanol selectivity	pervaporative dehydration	36
Santamaria et al.	2015	chitosan	fuel cell	concentration of chitosan, ratio of chitosan and phosphotungstic acid	membrane thickness, conductivity	hydrogen-oxygen fuel cell	37
Zhu et al.	2015	PES and PVP blended chitosan and montmorillonite	membrane separation	additive concentration	water flux, salts rejection	dyes purification	38
Li et al.	2015	chitosan	biomedical application	concentration of genipin as a cross-linker	swelling ratio, mechanical strength	cultivation medium of epithelial cells	39
Alias et al.	2015	chitosan blended SiO_2	membrane separation	mixing ration of chitosan and SiO_2	pore size, water uptake	proton battery	19
Hegab et al.	2015	chitosan	membrane separation	surface modification by using graphen oxide	hydrophilicity, NaCl rejection, water flux, antifouling activity	reverse osmosis	40
Zhang et al.	2015	poly (vinyl alcohol) blended chitosan	biomedical application	blending ratio of chitosan	mechanical strength, water vapor, oxygen permeability, antibacterial activity	wound dressing	41
Panda et al.	2015	chitosan coated iron-oxide-polyacrylonitrile	membrane separation	chitosan coating, concentration of Fe_3O_4	permeability, MWCO, pore size, hydrophilicity, mechanical strength	remove of humic acid	42
Antunes et al.	2015	chitosan and arginine	biomedical application	-	-	wound regeneration	43
Song et al.,	2015	chitosan containing carbon nanotube	antibacterial medium	blending ratio among chitosan, cationic chitosan, carbon nanotubes and silicon cuouple agent	hydrophobicity, mechanical strength	surface modification	44
Wang and He	2015	chitosan blended copolymer of polyacrylamide/polystyrene	fuel cell	blending ratio of chitosan and polyacrylamide/polystyrene	methanol permeability, wataer uptake, mecanical strength	methanol alkaline fuel cells	45
Malini et al.	2015	chitosan contained ZnO	antibacterial medium	combined with ZnO nano particules	antibacterial activity, antifouling activity	nanocomposite membrane	46

GTMAC: Glycidyltrimethylammonium chloride, PES: polyethersulfone, PDMCHEA:poly (2-methacryloyloxy ethyl trimethylammonium chloride-co-2-hydroxyethyl acrylate), PVP: polyvinylpyrrolidone

http://dx.doi.org/10.5772/61998

2.2.2. Water permeation flux

Figure 3 demonstrates that the water permeation flux and the volumetric void fraction of the swollen membrane were almost linearly correlated. The NaOH concentration in the neutralization process enhanced both the water permeation flux and the void fraction in the membrane. Neutralization using a high NaOH concentration weakens hydrogen bonding between chitosan polymer chains. The void fraction in the swollen membrane can assumed to be the volume of a water permeation channel occupying the membrane. This result suggests that the membrane structure involving water permeation was dominantly regulated by the NaOH concentration during neutralization.

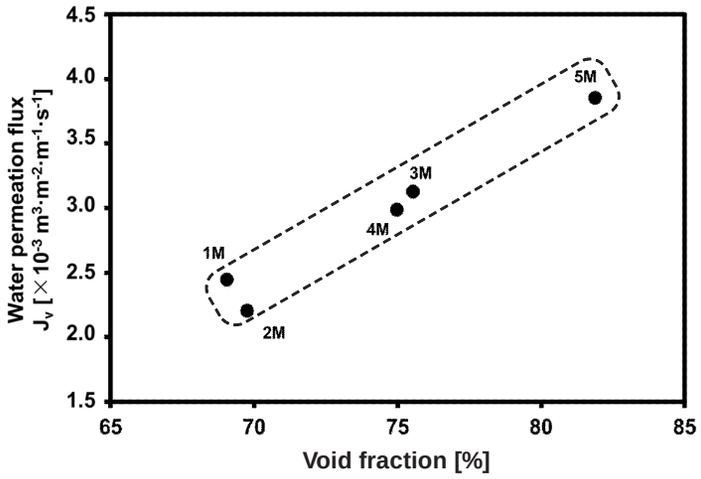

Figure 3. Correlation between the water permeation flux and the void fraction of 81% deacetylation degree chitosan membrane in reference [16]. The concentrations of NaOH used in the neutralization process are indicated at adjacent to keys, respectively.

2.2.3. Mass transfer characteristics

The effective diffusion coefficient of the model components was evaluated based on the mass transfer flux. The membrane was sandwiched between twin mass transfer cells. The feed solution contained the model components (urea 60 Da, Methyl Orange 327 Da, Rose Bengal 1017 Da, and Sirius Red 1373 Da) at the desired concentrations, and the stripping solution was deionized water. The overall mass transfer coefficient K_{OL} was evaluated from the mass transfer flux according to Eq. (2).

$$\ln\left(1-\frac{2C_s}{C_{fi}}\right)=-\frac{2AK_{OL}}{V}t \tag{2}$$

Here, C_s and C_{fi} are the concentrations of the stripping and initial feed solutions, A is the mass transfer area of the membrane, V is the volume of aqueous phase in each transfer cell, and t is the operation time.

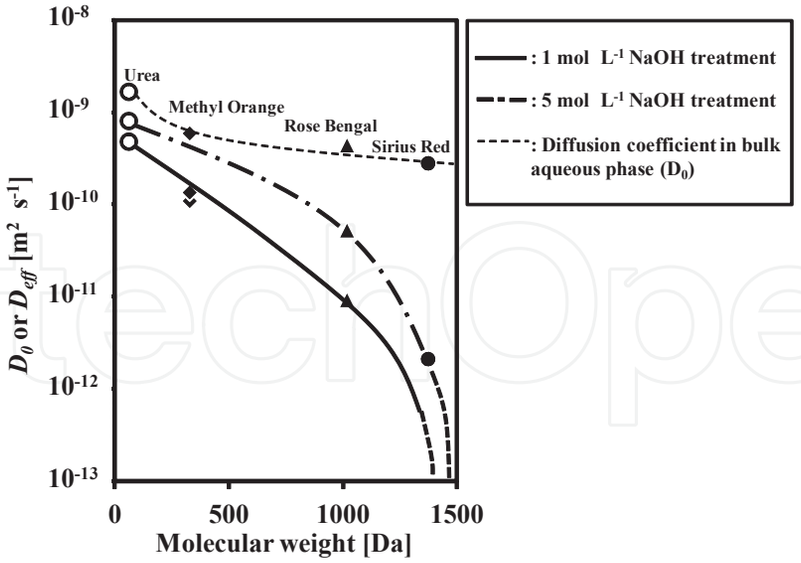

Figure 4. Change of effective diffusion coefficient (D_{eff}) versus molecular weight of tested components (81% deacetylation) [16].

The overall mass transfer coefficient K_{OL} included the film mass transfer resistances (k_{L1}^{-1} and k_{L2}^{-1}) and the membrane mass transfer coefficient (k_m) as seen in Eq. (3).

$$K_{OL}^{-1} = k_{L1}^{-1} + k_m^{-1} + k_{L2}^{-1} \tag{3}$$

The aqueous phases in the mass transfer cells were sufficiently stirred to attain a fully developed turbulent condition ($Re > 10^4$). The film mass transfer resistances (k_{L1}^{-1} andk_{L2}^{-1}) within the overall mass transfer resistance (K_{OL}^{-1}) were ignored under fully turbulent conditions. This directly indicated the membrane mass transfer coefficient (k_m). The effective diffusion coefficient was evaluated from k_m using Eq. (4):

$$k_m = \frac{D_{eff}}{\ell} \tag{4}$$

The initial membrane thickness in the swollen state (ℓ) was measured with a micrometer (Mitutoyo Corporation, Kanagawa, Japan).

Figure 4 depicts the change in the effective diffusion coefficient in the chitosan membrane with the molecular weight of the tested components for 81% *DD*. The effective diffusion coefficient of a chitosan membrane prepared from NaOH of 1mol·L^{-1} changed dramatically at a molecular size corresponding to Rose Bengal (1017 Da). This result suggested that the size distribution of the mass transfer channel in the membrane was monodisperse and similar to the molecular size of Rose Bengal.

The effective diffusion coefficient of a membrane prepared from 5 mol·L^{-1} NaOH greatly increased relative to a membrane prepared from 1 mol·L^{-1}. The molecular diffusion channel

http://dx.doi.org/10.5772/61998

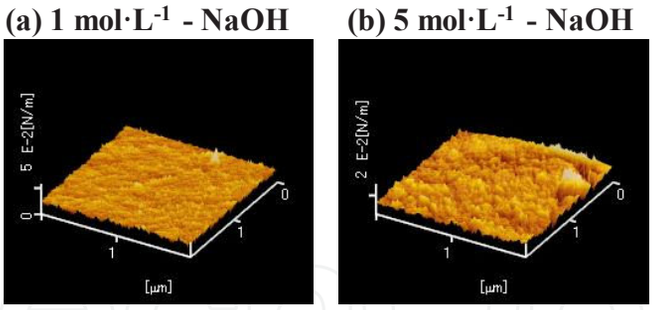

Figure 5. Scanning probe microscope photographs of chitosan membrane surface. (a) 1 mol L^{-1} NaOH, (b) 5 mol L^{-1} NaOH [16].

formed by the polymer networks became enlarged due to the higher NaOH concentration employed.

The dominant role of the acid–base neutralization process in chitosan membranes was revealed to control membrane properties involving mechanical strength, the water permeation flux, and the effective diffusion coefficient.

2.2.4. Morphology of chitosan membrane

Figure 5 presents scanning probe microscope (SPM) photographs of chitosan membrane surfaces. The chitosan membrane made from 1 mol·L^{-1} NaOH had a very smooth surface. In contrast, the membrane made from 5 mol·L^{-1} NaOH had a somewhat rough surface.

2.3. Other regulation factors

2.3.1. Deacetylation degree

The deacetylation degree (*DD*) of a chitosan membrane can be stoichiometrically controlled by an acetic anhydride additive. Effects of the deacetylation degree on membrane properties, such as water permeation flux, have been found [50]. The water permeation flux of a membrane prepared from 99.2% *DD* chitosan was remarkably enhanced about 100-fold compared with a 76.5% *DD* chitosan membrane. The water permeation flux increased exponentially with increasing deacetylation degree from 81.8% to 92.2% [51].

Increasing the deacetylation degree enhances the surface hydrophilicity of the membrane surface because the acetamido groups on the chitosan membrane are converted into amino groups. This advances the effective formation of hydrogen bonds between the amino and hydroxyl groups and between the amino groups in the chitosan molecules, thus resulting in a dense molecular chain in the membrane [18].

2.3.2. Molecular weights of chitosan

Chitosan membranes prepared by Uragami and coworkers from different molecular weights (13–201 kDa) were tested during pervaporation dehydration of an ethanol aqueous solution.

The permeation flux decreased with increasing molecular weight from 13 kDa to 90 kDa, then increased from 90 kDa to 201 kDa. In contrast, the water permeation selectivity from the ethanol aqueous solution increased remarkably with increasing molecular weight up to 90 kDa. Over 90 kDa, the selectivity decreased. These results were understood to indicate that the 90 kDa molecular weight effectively formed entanglements and thus produced the strongest hydrogen bonds between the molecular chains of chitosan [18], although the mechanical strength increased with increasing average molecular weight of chitosan [52].

2.3.3. Addition of a cross-linker

Basically, chitosan can be formed into an insoluble membrane by acid–base neutralization in the casting solution without using a cross-linker. However, the addition of a cross-linker to improve membrane characteristics was carefully investigated.

The most prominent effect of an additive cross-linker is improved mechanical strength. Figure 6 depicts the change of mechanical strength of chitosan membrane (maximum stress vs. maximum strain at membrane rupture) with increasing amount of cross-linker. In a common trend, increasing the amount of cross-linker forms a rigid membrane. The addition of genipin as a cross-linker increased the maximum stress and reduced the maximum strain at membrane rupture [39]. Increasing added amounts of glutaraldehyde, methanol with ethylene glycol diglycidyl ether, and gallic acid also increased the mechanical strength. However, excess addition of cross-linker formed rigid and fragile structures on the chitosan membrane [25–26, 53].

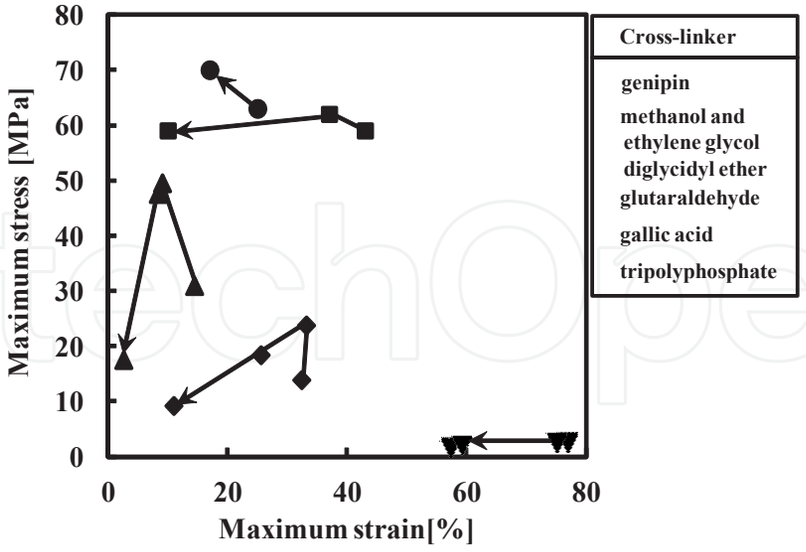

Figure 6. Change of mechanical strength of chitosan membranes with increasing amount of cross-linker. ●: chitosan membrane cross-linked with genipin [54]. ■: chitosan membrane cross-linked with methanol and ethylene glycol diglycidyl ether [53]. ▲: chitosan membrane cross-linked with glutaraldehyde [25]. ◆: chitosan membrane cross-linked with gallic acid [26], ▼: chitosan cross-linked with tripolyphosphate [55]. Arrows indicate increasing additive amount of each cross-linker.

http://dx.doi.org/10.5772/61998

Other researchers have reported that cross-linking with sodium tripolyphosphate enhanced the mechanical strength of chitosan membrane [17]. From another viewpoint, Shenvi and coworkers determined the effect of the pH value of the cross-linking solution on the membrane properties. A chitosan membrane cross-linked by tripolyphosphate solution at pH 5 realized a higher rejection rate of NaCl and $MgSO_4$ than a membrane cross-linked at pH 9 [28].

The enhancement of pervaporative dehydration ability of water–alcohol mixtures by adding cross-linker has been frequently reported [56]. A chitosan membrane cross-linked with toluene-2,4-diisocyanate exhibited high pervaporative dehydration ability with an isopropanol aqueous solution in which the selectivity of water α was performed as 472 [57]. The selectivity of water α was calculated using the following equation:

$$\alpha = \frac{y\,(1-x)}{x\,(1-y)} \tag{5}$$

Here, y is the permeate weight fraction of water and x is the feed weight fraction of water.

2.3.4. Hybrid approaches with other materials

Some hybrid approaches using chitosan and other materials have been proposed to overcome problems in practical use [35]. To make a porous structure on a chitosan membrane, SiO_2, a porogen agent, was mixed with chitosan cast solution and removed from the membrane. The average pore size reached a maximum of 8.5 μm when the mixing ratio of chitosan and SiO_2 was 1:2 [19].

Chitosan membranes are frequently combined with nanomaterial to form a composite medium. A chitosan membrane composited with a multi-walled carbon nanotube was modified by adding perfluorooctanesulfonyl fluoride (PFOSF). The added PFOSF enhanced antibacterial activity due to its remarkable hydrophobicity. The mechanical strength increased with increasing multi-walled carbon nanotubes [44]. Chitosan composited with ZnO nanoparticles was also investigated for antibacterial activity [46]. Chitosan membrane has a good potential as a composited nanomaterial medium for biologically based nanotechnology.

2.3.5. Chemical modification of the chitosan molecular chain

Chitosan has great potential for chemical modification. Functionalized chitosan is often used as the main membrane body, coating agent, or additive agent for functionalization of surface modifications. Graphene oxide functionalizing a chitosan membrane as a surface modification agent on a commercial polyamide membrane has been investigated. The water flux and NaCl rejection of the chitosan membrane were increased by the modification, due to the formation of a dense, thin layer of graphene-oxide-functionalized chitosan, which is better than natural chitosan membrane [40]. Kumar and coworkers prepared various chitosan membranes: a natural chitosan blended with polysulfone membrane, an *N*-succinylchitosan blended with polysulfone membrane, and an *N*-propylphosphonyl

chitosan blended with polysulfone membrane. These membranes were applied to a heavy metal purification process. *N*-succinylchitosan blended with polysulfone membrane sufficiently purified Cu, Ni, and Cd [32].

3. Alginate membrane

Alginate is abundantly and sustainably produced by marine biological resources, especially brown seaweed. It has been widely applied in the food industry [58] and as a thickener [59], a suspending agent [60], an emulsion stabilizer [61], a gelling agent [62], and a film-forming agent [63]. In addition, alginate was continuously developed as useful materials for biomedical applications, especially for controlled delivery of drugs and other biologically active compounds and for the encapsulation of cells [64]. In recent pioneering works, alginate has developed as membrane material with excellent molecular selectivity for water-soluble components [65]. Recent studies of various alginate membranes are listed in Table 4 and Table 5 referred to previous literatures [10-11, 15, 22, 66-95].

3.1. Chemical composition and membrane formation of alginate

The molecular chain of alginate is constructed of a block copolymer of β-D-mannuronate (Figure 7a) and α-L-guluronate (Figure 7b) [96]. These two uronates construct a polymeric block in an alginate polymer chain with the following three types of block: homopolymeric blocks of α-L-guluronate (GG blocks), blocks with an alternating sequence in varying proportions of guluronate and mannuronate (MG blocks), and homopolymeric blocks of β-D-mannuronate (MM blocks) [97]. GG blocks chelate alkaline earth-metal ions because of the spatial arrangement of the pyranose ring and the hydroxyl oxygen atoms, and thus create a much stronger interaction than MM blocks and MG blocks [98–99].

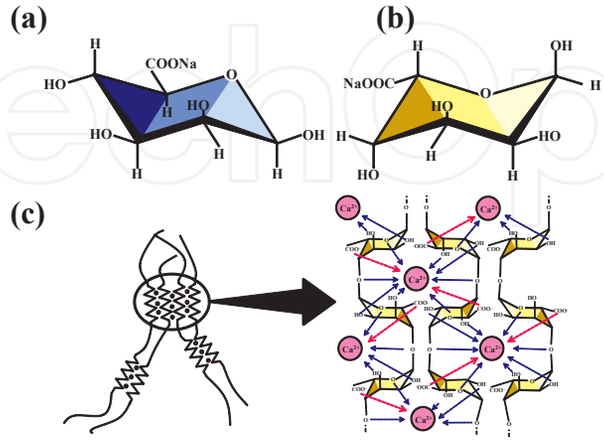

Figure 7. Residues of alginate molecular chain. (a) β-D-mannuronate. (b) α-L-guluronate. (c) Chelation of homopolymeric blocks of α-L-guluronate junction with calcium ions. Alginate was cross-linked by divalent cations according to the "Egg-box" model.

http://dx.doi.org/10.5772/61998

Kashima, Nomoto and Imai 2015.

Table 4. Recent investigations of alginate membrane (2004–2013).

Authors	Year	Membrane material	Application	Raguration factor	Controled properties of membrane	Coments	Ref.
Toti and Aminabhavi	2004	sodium alginate	membrane separation	containing ratio of PVA and PEG	swelling ratio, water permeability, water/isopropanol selectivity	pervaporative dehydration	66
Kalyani et al.	2008	sodium alginate	membrane separation	with or without phosphoric acid as a cross-linker	swelling ratio, water permeation flux, water/ethanol selectivity	pervaporative dehydration	67
Kashima and Imai	2010	calcium alginate	membrane separation	concentration of $CaCl_2$ as a cross-linker	mechanical strength, swelling ratio, water permeation flux, effective diffusion coefficient	mass transfer characteristics	10
Saraswathi et al.	2011	calcium alginate blended dextrin	membrane separation	blending ratio of alginte and dextrin	swelling ratio, water permeability, water/isopropanol selectivity	pervaporative dehydration	68
Li et al.	2011	sodium alginate blended gelatin	membrane separation	blending ratio of gelatin	crystallinity, water uptake, water permeability, water/C_3H_6 selectivity	hollow fiber	69
Taskin et al.	2011	sodium alginate photografted with itaconic acid	material science	grafting time and temperture, concentration of benzophenone	swelling ratio, hydrophilicity	hydrophilic material	70
Chen et al.	2011	sodium alginate containing humic acid	membrane separation	containing humic acid	adsorption ability of Cu(II)	adsorption of Cu(II)	71
Kashima and Imai	2011	calcium alginate	membrane separation	homopolymeric blocks of α-L-guluronate	mechanical strength void fraction, mass transfer characteristics	mass transfer characteristics	11
Li et al.	2012	sodium alginate blended PVA and PSf	membrane separation	blending ratio of PVA	crystallinity, water uptake, water vapor flux	dehumidification	72
Nigiz et al.	2012	sodium alginate containing zeolite	membrane separation	containing ratio of zeolite	water permeation flux, water/ethanol selectivity	pervaporative dehydration	73
Sajjan et al.	2013	sodium alginate blended chitosan-wrapped MWCNTs	membrane separation	blending ratio of chitosan-wrapped MWCNTs	swelling ratio, permation flux, water/isopropanol selectivity	pervaporative dehydration	74
Flynn et al.	2012	sodium alginate blended PVA	membrane separation	membrane thickness	permeation flux, water/ethanol selectivity	pervaporative dehydration	75
Shi et al.	2013	calcium alginate containing $CaCO_3$, PAA and PUA	drug release	containing with or without $CaCO_3$, PAA and PUA	swelling ratio, drug release ability	biomineralization	76
Chen et al.	2013	sodium algiante containing APTEOS	membrane separation	containing APTEOS	adsorption ability of Cr(III)	adsorption of Cr(III)	77
Zhu et al.	2013	sodium alginate	membrane separation	concentration of sodium tartrate as a cross-linker	CO_2 permeability, CO_2/N_2 selectivity	CO_2 separation	78
Adoor et al.	2013	sodium alginate containing phosphotungstic acid	membrane separation	containing ratio of phosphotungstic acid	water permeation flux, water/ethanol and water/isopropanaol selectivity	pervaporative dehydration	79
Moraes et al.	2013	alginate blended chitosan	membrane separation	blended chitosan	swelling ratio, thickness, adsorption of herbicide	water treatment	15

APTEOS: 3-aminopropyltriethoxysilane, MWCNTs: multiwalled cabon nanotubes, PAA: polyacrylic acid, PAN: polyacrylonitrile, PEG: polyethylene glycol, PSf: polysulfone, PUA: poly (urethane-amine), PVA: poly (vinyl alcohol),

Table 5. Most recent investigations of alginate membrane (2014–2015).

Authors	Year	Membrane material	Application	Raguration factor	Controled properties of membrane	Coments	Ref.
Zhang et al.	2014	sodium alginate supported on polypropylene	membrane separation	kind of cross-linking metal ion	mechanical strength, hydrophilicity, permeation flux, water/acetic acid selectivity	pervaporative dehydration	80
Gao et al.	2014	sodium alginate and hyaluronic acid supported on PAN	membrane separation	concentration of Ca^{2+} as a cross-linker, coating sequence of alginate and hyaluronic acid	swelling ratio, hydrophilicity, permeation flux, water/ethanol selectivity	pervaporative dehydration	81
Kuila and Ray	2014	sodium alginate blended PVA	membrane separation	blending ratio of alginate and PVA	mechanical strength, permeation flux, water/dioxane selectivity	pervaporative dehydration	82
Kuila and Ray	2014	sodium alginate blended CMC	membrane separation	blending ratio of alginate and CMC	permeation flux, benzene/cyclohexan selectivity	pervaporative separation	83
Yang et al.	2014	sodium alginate blended PVA	fuel cell	blending ratio of sodium alginate and PVA, time of crosslinking with glutaraldehyde	swelling ratio, ionic conductivity, methanol permeability	direct methanol fuel cell	84
Cabello et al.	2014	alginate blended carrageenan	fuel cell	blending ratio of alginate and carrageenan	mechanical strength, water uptake, proton conductivity, methanol permeation flux	direct methanol fuel cell	85
Cao et al.	2014	sodium alginate containing graphene oxides	membrane separation	containing ratio of graphene oxides	hydrophilicity, crystallinity, swelling ratio, permeation flux, water/ethanol selectivity	pervaporative dehydration	86
Yoo and Ghosh	2014	calcium alginate	biomedical application	concentration of alginate and $CaCl_2$, cross-linking time	membrane thickness	microporous hollow fiber	87
Kamoun et al.	2015	sodium alginate blended PVA	biomedical application	blending ratio of sodium alginate and PVA	water uptake, mechanical strength, release property, adsorption of BSA	wound dressing	88
Li et al.	2015	calcium alginate	biomedical application	concentration of ethanol as solvent of $CaCl_2$	swelling ratio, thickness, mechanical strength	pharmaceutical products	89
Zhang et al.	2015	calcium alginate blended polyacrylamide	membrane separation	with or without polyacrylamide	water permeation flux, adsorption of BSA (antifouling activity), rejection of Brilliant Blue	nanofiltration	22
Saozo et al.	2015	calcium alginate	edible film	concentration of alginate and calcium gluconolactate, heat treatment	thickness, mechanical strength, color	membrane preparation	90
Zhao et al.	2015	calcium alginate	membrane separation	concentration of sodium alginate, modification by PEG	water permeation flux, rejection of PEG and methylene blue, antifouling activity	ultrafiltration, nanofiltration	91
Jie et al.	2015	calcium alginate containing carbon nanotubes	membrane separation	containing ratio of carbon nanotubes	mechanical strength, antifouling activity, water permeation flux, dye rejection	nanofiltration	92
Kirdponpattara et al	2015	alginate blended cellulose	biomedical application	blending alginate and bacterial cellulose	pore size, void fraction, mechanical strength, biocompatibility	tissue enginering	93
Shao et al.	2015	sodium alginate blended cellulose loaded with AgSD	biomedical application	loaded ratio of AgSD	swelling ratio, antibacterial ability	wound dressing	94
Uragami et al.	2015	alginate blended DNA	membrane separation	kind of cross-linking metal ion	hydrophilicity, swelling ratio, density, water/ethanol selectivity	pervaporative dehydration	95

AgSD: silver sulfadiazine, CMC: carboxymethyl cellulose, DNA: deoxyribonucleic acid, PEG: polyethylene glycol, PVA: poly (vinyl alcohol),

http://dx.doi.org/10.5772/61998

Sodium alginate easily forms a cross-link with the presence of divalent cations such as Ca^{2+}, resulting in a highly compacted and dense gel network. GG blocks are constructed mainly of a cross-linked zone with Ca^{2+}. This is called an "Egg-box junction" (Figure 7c), where the ions were assimilated to "Eggs" [100].

Sodium alginate forms a cross-link in the presence of divalent cations such as Ca^{2+}, resulting in a highly compacted gel network. Homopolymeric blocks of α-L-guluronate are constructed mainly of a cross-linked zone with divalent cations. This section describes the impact of this kind of divalent cations and the mass fraction of homopolymeric blocks of α-L-guluronate in an alginate polymer chain (F_{GG}).

The authors previously reported the preparation of alginate membrane described below [10–11]. A 20 mL sodium alginate aqueous solution (10 $g \cdot L^{-1}$) was placed in a Petri dish. The solution was gradually dried at a mild temperature in a desiccator (298 K) or an electrical dryer (303 K) for 24 h to prevent heat degradation. A dried, thin film of sodium alginate was obtained on the Petri dish.

An electrolyte aqueous solution ($CaCl_2$, $SrCl_2$, and $BaCl_2$) was directly introduced onto the dried, thin sodium alginate film as a source of divalent cation for cross-linking. The concentration range of the electrolyte aqueous solutions was 0.1–1.0 $mol \cdot L^{-1}$. A stable alginate membrane was quickly formed in the Petri dish at room temperature. After 20 min, the prepared swollen membrane was spontaneously separated from the surface of the Petri dish. The membrane remained in the electrolyte aqueous solution for further 20 min. The membrane was totally immersed in the electrolyte aqueous solution for 40 min. The prepared membrane was repeatedly washed with pure water to remove excess electrolyte, and then stored in pure water.

3.2. Effect of homopolymeric block of α-L-guluronate (F_{GG})

The authors previously reported that membrane properties are evidently controlled by the mass fraction (F_{GG}) [11, 65, 101]. At first, the mass of GG blocks in the actual alginate polymer chain was determined by acid hydrolysis combined with Bitter–Muir's carbazole sulfuric acid method [102]. The actual alginate was separated into three fractions (GG block, MM block, and MG block) by the acid-hydrolysis method. Acid-hydrolysis protocols were employed according to a previously published method [11, 103]. Their obtained fractions were then determined by Bitter–Muir's carbazole sulfuric acid method using an optical density of 530 nm (UV-1200, Shimadzu, Kyoto, Japan). The calibration curve for mannuronic acid lactone was obtained and used as the standard component of uronic acid. These methods produced good intensity and accuracy of coloration [104].

The mass of the GG block (W_{GG}) was obtained from a fractional solution of the GG block by acid hydrolysis. The masses of the MM block (W_{MM}) and MG block (W_{MG}) were determined in the same way. The mass fraction of the homopolymeric blocks of α-L-guluronate (F_{GG}) was then calculated using the following formula:

$$F_{GG} = \frac{W_{GG}}{W_{GG} + W_{MM} + W_{MG}} \tag{6}$$

F_{GG} was therefore shown to be a key factor in regulating membrane properties. In this study, two sodium alginates were examined, F_{GG} 0.18 and F_{GG} 0.56. Calcium alginate membrane prepared from five types of sodium alginate (F_{GG} 0.18, 026, 0.35, 0.45, and 0.56) were regulated by mixing with two types of sodium alginate (F_{GG} 0.18 and 0.56).

3.2.1. Mechanical strength

The effect of F_{GG} on mechanical strength is depicted in Figure 8. The mechanical strength was determined based on the membrane deformation. The maximum stress was defined at the rupture of the membrane. This value increased with increasing F_{GG}. In contrast, the maximum strain decreased with increasing F_{GG}. The mechanical properties of the calcium alginate membrane changed from elastic to plastic transfer, depending on F_{GG}.

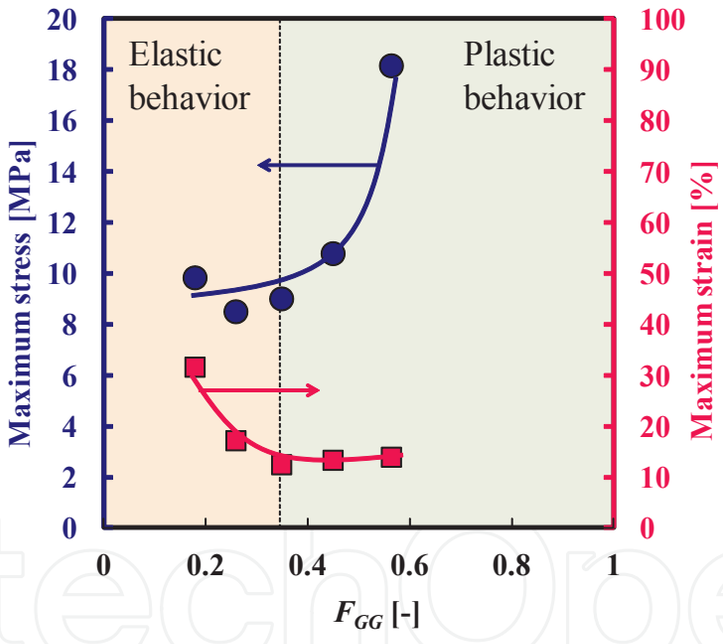

Figure 8. Effect of F_{GG} on mechanical strength of calcium alginate membrane [11].

3.2.2. Mass transfer characteristics

An alginate membrane performs superior molecular size recognition on low-molecular-weight components from 60 Da to 600Da [10]. Figure 9 demonstrates that the effective diffusion coefficient in the membrane (D_{eff}) of saccharides (glucose, G, 180Da; maltose, M, 324 Da; raffinose, R, 504 Da) can be efficiently changed by regulating F_{GG}. The effective diffusion coefficient in the membrane prepared from F_{GG} 0.56 alginate was proportional to the –4.6th power of the molecular volume. The diffusion coefficient in bulk aqueous phase (D_0) was

http://dx.doi.org/10.5772/61998

inversely proportional to the 0.6th power of the molecular volume [105]. In contrast, the effective diffusion coefficient in the membrane prepared from F_{GG} 0.18 alginate was proportional to the –2.9th power of the molecular volume. The higher F_{GG} membrane exhibited more sensitive molecular size recognition. "Egg-box junction" zones constructed from calcium ions and homopolymeric blocks of α-L-guluronate dominantly regulated the mass transfer mechanism of the alginate membrane.

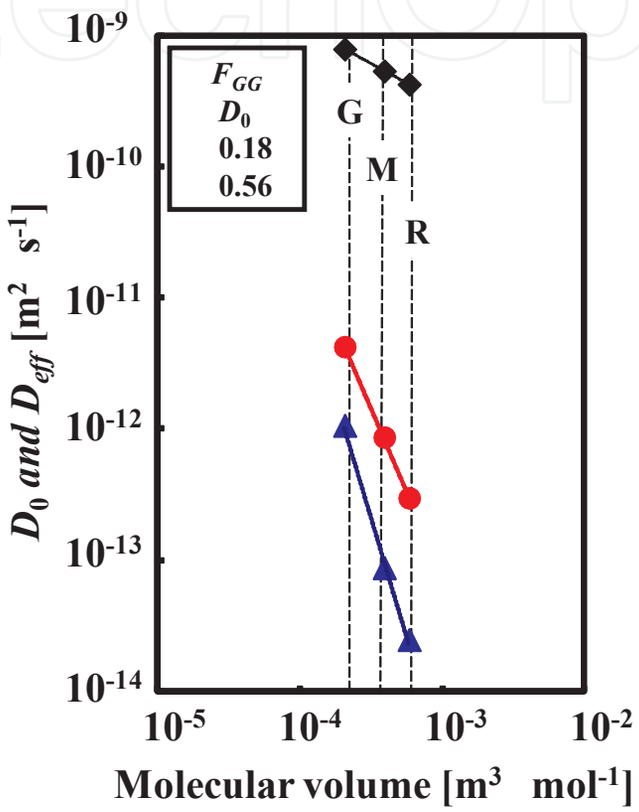

Figure 9. The effective diffusion coefficient changed remarkably in our experimental range from 180 Da to 504 Da. The symbol ◆ indicates the diffusion coefficient in bulk aqueous solution. Temperature: 303 K. Agitation rate: 14.2 s^{-1} [65].

The effect of F_{GG} on the mass transfer characteristics was evaluated using a permeation test with urea aqueous solution as a typical molecule model. The effective diffusion coefficient (D_{eff}) of urea in the membrane decreased with increasing F_{GG}. Figure 10 illustrates the correlation of the volumetric void fraction of the swollen membrane with the ratio between the effective diffusion coefficient of urea in the membrane and the diffusion coefficient in bulk aqueous phase (D_0). Both the effective diffusion coefficient and the volumetric water fraction were restrained by increasing F_{GG}. The strong dependency of the effective diffusion coefficient of urea on the void fraction contributes to good understanding of the formation of a mass transfer channels in the alginate membrane. These channels are speculated as being monodisperse in a similar size with urea molecule. The mass transfer channel was governed by the mass fraction of homopolymeric blocks of α-L-guluronate (F_{GG}).

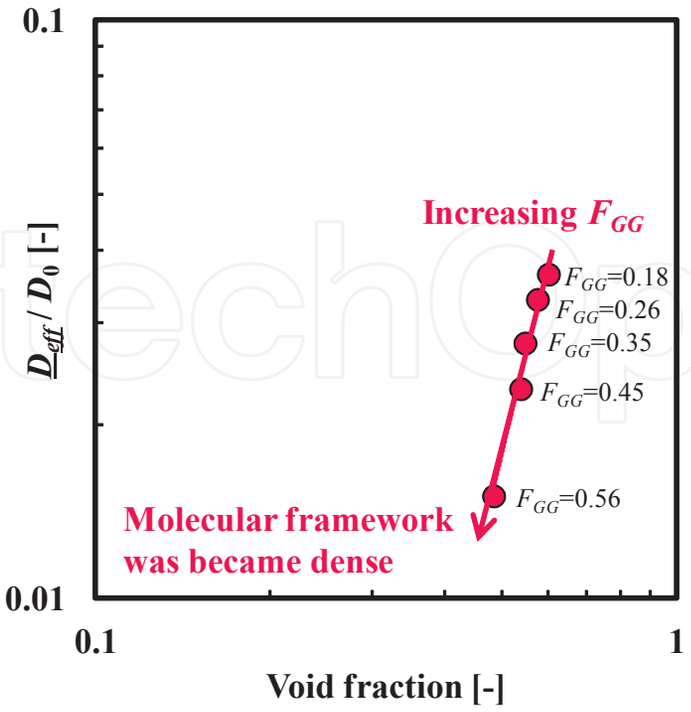

Figure 10. Correlation of the volumetric void fraction of the swollen membrane with the effective diffusion coefficient of urea [11].

3.2.3. Morphology of the alginate membrane

Figure 11 presents SPM photographs of the calcium alginate membrane surface. The distribution of membrane asperity clearly decays with increasing F_{GG}. Especially in higher F_{GG} conditions, many of the GG blocks formed a higher population density of Egg-box junction chelating with Ca^{2+}, and the atomic force of the polymer networks was uniform.

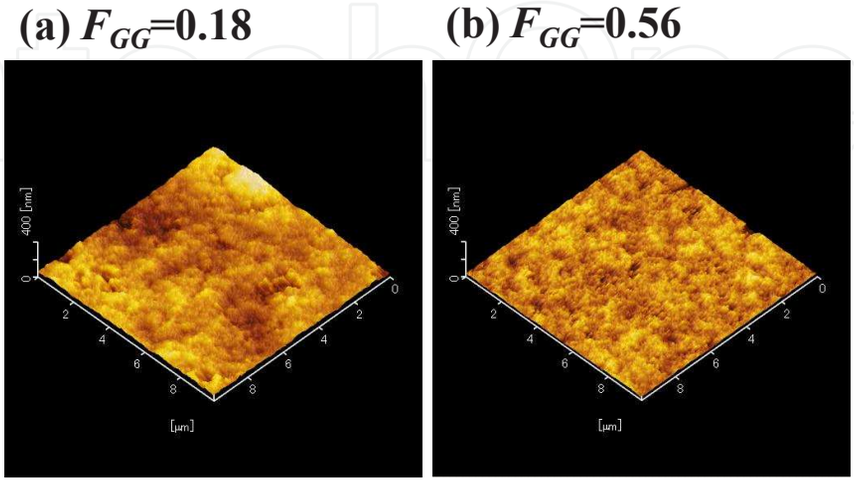

Figure 11. Scanning probe microscope photographs of calcium alginate membrane surface. (a) F_{GG} = 0.18, (b) F_{GG} = 0.56.

http://dx.doi.org/10.5772/61998

3.3. Effect of cross-linking divalent cations

The authors prepared a stable alginate membrane cross-linked with $CaCl_2$, $SrCl_2$, and $BaCl_2$. These membranes are sufficiently stable in aqueous phase to apply for practical use.

3.3.1. Water permeability

The water permeation coefficient was evaluated based on the pure water permeation flux as presented in Figure 12. It was decreased logarithmically with increasing concentration of cross-linker. This suggests that the number of permeation channels and/or the size of the permeation channels decreased with increasing concentration of cross-linking ions. The effect of cross-linker concentration on water permeability appeared strongly in the $BaCl_2$ used, suggesting that Ba^{2+} structures have a much stronger interaction in α-L-guluronate block. Binding of divalent cation to the three kind of copolymer blocks have been investigated [106–107]. The following orders of binding strength indicated by sign of equality were reported:

GG block: Ba > Sr> Ca >> Mg
MM block: Ba > Sr ≈ Ca ≈ Mg
MG block: Ba ≈ Sr ≈ Ca ≈ Mg

Hence, the alginate membrane cross-linked with $BaCl_2$ constructed a dense polymer network due to strong bonding between alginate molecular chain and Ba^{2+}.

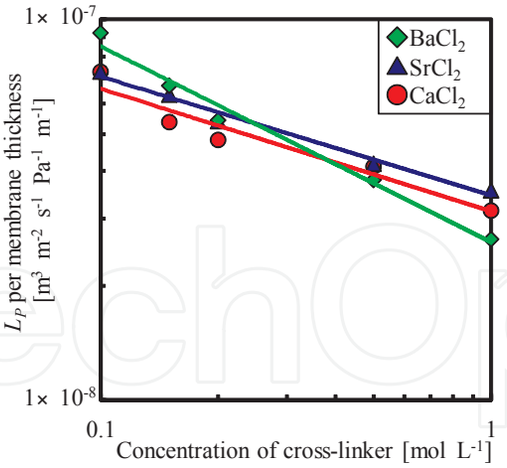

Figure 12. Effect of concentration of cross-linking electrolyte solution on water permeation coefficient.

3.3.2. Volumetric water fraction

The volumetric water content of a swollen membrane can be assumed to an indicator of the void fraction of the membrane structure [108]. Figure 13 illustrates the effect of the concentration of electrolyte solution on the void fraction of the membrane. The void fraction decreased

with increasing concentration of the cross-linking electrolyte solution. An alginate membrane cross-linked with $BaCl_2$ was highly densified by the provided Ba^{2+}.

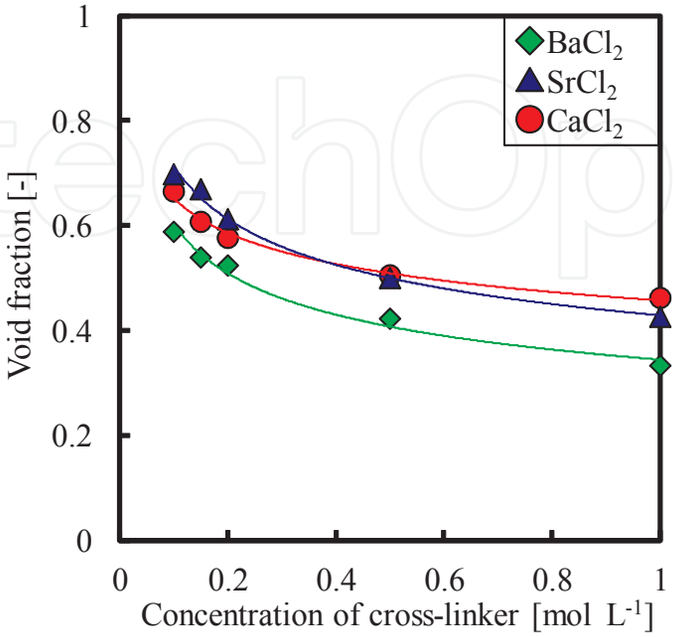

Figure 13. Effect of concentration of cross-linking electrolyte solution on void fraction of swollen alginate membrane.

3.4. Other regulation factors for controlling membrane properties

3.4.1. Addition of cross-linker other than metal ions

Conventional cross-linkers forming a polymer membrane were also examined to realize the alginate membrane. Glutaraldehyde is most commonly employed as a cross-linker to form sodium alginate membranes [83–84]. These membranes cross-linked with glutaraldehyde were developed for use in organic dehydration by pervaporation [66, 79, 82]. A sodium alginate membrane cross-linked with phosphoric acid was prepared for pervaporative dehydration of ethanol aqueous solution [67]. This resulted in 3.5×10^{-2} kg·m^{-2}·h^{-1} of permeation flux and 2182 of selectivity as defined by Eq. (4). A sodium alginate membrane cross-linked by sodium tartrate was characterized by CO_2 capture from CO_2/N_2 [78].

3.4.2. Hybrids with other polymers or materials

Many efforts have been made to enhance the performance of the alginate membrane by blending it with different hydrophilic polymers. An alginate-blended DNA membrane cross-linked with Mg^{2+} or Ca^{2+} was investigated with regard to the permeation flux of ethanol aqueous solution for pervaporation [95]. The permeation flux and selectivity of a calcium alginate membrane with DNA in pervaporative dehydration for an ethanol aqueous solution were measured as 1.2×10^{-2} kg·m^{-2}·h^{-1} and 5500, respectively. In contrast, a magnesium alginate

http://dx.doi.org/10.5772/61998

membrane with DNA exhibited a permeation flux and selectivity of 1.2×10^{-2} kg·m^{-2}·h^{-1} and 6500.

Hybrid membranes of sodium alginate and dextrin cross-linked with glutaraldehyde had a permeation flux of 9.65×10^{-2} kg·m^{-2}·h^{-1} permeation flux and a selectivity of 8991 in pervaporative dehydration for an isopropanol aqueous solution [68].

Alginate membranes are frequently combined with nanomaterials to form a composite medium. A calcium alginate membrane containing multi-walled carbon nanotubes was prepared as a new nanofiltration membrane. It had high mechanical strength, antifouling ability, and high rejection of small organic molecules (Congo Red, 697Da) [92].

4. Conclusion

Strategic regulation of an oceanic biopolymer membrane to control its characteristics in membrane separation technology was demonstrated. An oceanic biopolymer chitosan membrane can be easily prepared by casting chitosan in dilute aqueous organic acids and neutralizing it with an alkaline aqueous solution. The dominant role of neutralization for chitosan membrane involves the mechanical strength, the permeation flux, and the mass transfer characteristics. Other regulating factors, such as the deacetylation degree, the average molecular weight, and the addition of a cross-linker were presented.

A calcium alginate membrane performs superior molecular size recognition on low-molecular-weight components from 60 Da to 600 Da due to a dense polymer network consisting of homopolymeric blocks of α-L-guluronate and calcium ions. The kind of cross-linking ion used is also able to control the membrane properties. Barium ion performed a stronger cross-linker in the alginate membrane rather than Ca^{2+} and Sr^{2+}, and a highly complex structure was formed. The mass fraction of homopolymeric blocks of α-L-guluronate and cross-linking metal ions were impact factors in regulating the mass transfer characteristics, water permeability, and mechanical strength.

These oceanic polymers are biodegradable, biocompatible, environmentally friendly, stable, and easily available from renewable agricultural resources. In the future, oceanic biopolymer membranes should be developed as an alternative to artificial polymer membranes.

Nomenclature

A Area of membrane surface [m^2]

C_{fi} Initial concentration in the feed solution [mol·L^{-1}]

C_s Concentration in the stripping solution [mol·L^{-1}]

D_0 Diffusion coefficient in a bulk aqueous phase estimated from Wilke–Chang's empirical formula [m^2·s^{-1}]

DD Deacetylation degree [%]

D_{eff} Effective diffusion coefficient [$m^2 \cdot s^{-1}$]

F_{GG} Mass fraction of GG block inalginate determined by Eq. (5) [–]

K_{OL} Overall mass transfer coefficient [$m \cdot s^{-1}$]

K_{OL}^{-1} Overall mass transfer resistance [$(m \cdot s^{-1})^{-1}$]

k_m Membrane mass transfer coefficient [$m \cdot s^{-1}$]

k_{L1} Film mass transfer coefficient in the feed phase [$m \cdot s^{-1}$]

k_{L2} Film mass transfer coefficient in the stripping phase [$m \cdot s^{-1}$]

ℓ Membrane thickness in the initial state [m]

n_{AGS} Molar number of acetylglucosamine residues in polymer chain of chitin or chitosan [mol]

n_{GS} Molar number of glucosamine residues in polymer chain of chitin or chitosan [mol]

Re Reynolds number [–]

t Time [s]

V Volume of aqueous solution in the transfer cell [m^3]

W_{GG} Mass of GG block in sodium alginate [kg]

W_{MG} Mass of MG block in sodium alginate [kg]

W_{MM} Mass of MM block in sodium alginate [kg]

x Feed weight fraction of water in pervaporation [–]

y Permeate weight fraction of water in pervaporation [–]

α separation factor on pervaporative dehydration defined by Eq. (4) [–]

Author details

Keita Kashima[1], Ryuhei Nomoto[2] and Masanao Imai[2*]

*Address all correspondence to: XLT05104@nifty.com

1 Department of Materials Chemistry and Bioengineering,National Institute of Technology, Oyama College, Oyama, Tochigi, Japan

2 Course in Bioresource Utilization Sciences,Graduate School of Bioresource Sciences, Nihon University, Fujisawa, Kanagawa, Japan

References

[1] Xiong B, Richard T L, Kumar M. Integrated acidogenic digestion and carboxylic acid separation by nanofiltration membranes for the lignocellulosic carboxylate platform. J. Membrane Science. 2015;489: 275–283. DOI: 10.1016/j.memsci.2015.04.022

[2] Xiao T, Wang P, Yang X, Cai X, Lu J. Fabrication and characterization of novel asymmetric polyvinylidene fluoride (PVDF) membranes by the nonsolvent thermally induced phase separation (NTIPS) method for membrane distillation applications. J. Membrane Science. 2015;489: 160–174.DOI: 10.1016/j.memsci.2015.03.081

[3] Sawada S, Ursino C, Galiano F, Simone S, Drioli E, Figoli A. Effect of citrate-based non-toxic solvents on poly (vinylidene fluoride) membrane preparation via thermally induced phase separation. J. Membrane Science. 2015;493: 232–242. DOI: 10.1016/j.memsci.2015.07.003

[4] Baker R W. Membrane Technology and Applications. 3rd ed. Chichester: John Wiley & Sons Ltd; 2012. 575p. DOI: 10.1002/9781118359686

[5] Ma B, Qin A, Li X, Zhao X, He C. Structure and properties of chitin whisker reinforced chitosan membranes. International J. Biological Macromolecules. 2014;64: 341–346. DOI:10.1016/j.ijbiomac.2013.12.015

[6] Bueno C Z., Dias A M A, de Sousa H J C, Braga M E M, Moraes A M. Control of the properties of porous chitosan-alginate membranes through the addition of different proportions of Pluronic F68. Materials Science and Engineering C 2014;44: 117–125. DOI: 10.1016/j.msec.2014.08.014

[7] Loeb S, Sourirajan S. Sea water demineralization by means of an osmotic membrane. In: Advances in Chemistry. Vol. 38.America: ACS Publications; 1963. p. 117–132. DOI: 10.1021/ba-1963-0038.ch009

[8] Wu P, Imai M. Novel biopolymer composite membrane involved with selective mass transfer and excellent water permeability. In: Ning R Y, editor. Advancing Desalination. Croatia: InTech; 2012. p. 57–81. DOI: 10.5772/50697

[9] Torres F G, Troncoso O P, Piaggio F, Hijar A. Structure–property relationships of a biopolymer network: The eggshell membrane. Acta Biomaterialia. 2010;6: 3687–3693. DOI: 10.1016/j.actbio.2010.03.014

[10] Kashima K, Imai M, Suzuki I. Superior molecular size screening and mass-transfer characterization of calcium alginate membrane. Desalination and Water Treatment. 2010;17: 143–149. DOI: 10.5004/dwt.2010.1710

[11] Kashima K, Imai M. Dominant impact of the α-L-guluronic acid chain on regulation of the mass transfer character of calcium alginate membranes. Desalination and Water Treatment. 2011;34: 257–265. DOI: 10.5004/dwt.2011.2892

[12] Michalak I, Mucha M. The release of active substances from selected carbohydrate biopolymer membranes. Carbohydrate Polymers. 2012;87: 2432–2438. DOI: 10.1016/j.carbpol.2011.11.013

[13] Wu P, Imai M. Excellent dyes removal and remarkable molecular size rejection of novel biopolymer composite membrane. Desalination and Water Treatment. 2013;51: 5237–5247. DOI: 10.1080/19443994.2013.768836

[14] Lakra R, Saranya R, Lukka Thuyavan Y, Sugashini S, Meera K M, Begum S, Arthanareeswaran G. Separation of acetic acid and reducing sugars from biomass derived hydrosylate using biopolymer blend polyethersulfone membrane. Separation and Purification Technology. 2013;118: 853–861. DOI: 10.1016/j.seppur.2013.08.023

[15] Moraes M A, Cocenza D S, Vasconcellos F da C, Fraceto L F, Beppu M M. Chitosan and alginate biopolymer membranes for remediation of contaminated water with herbicides. J. Environmental Management. 2013;131: 222–227. DOI: 10.1016/j.jenvman.2013.09.028

[16] Nomoto R, Imai M. Dominant role of acid-base neutralization process in forming chitosan membrane for regulating mechanical strength and mass transfer characteristics. J. Chitin and Chitosan Science. 2014;2: 197–204. DOI: 10.1166/jcc.2014.1055

[17] Ma S, Chen Z, Qiao F, Sun Y, Yang X, Deng X, Cen L, Cai Q, Wu M, Zhang X, Gao P. Guided bone regeneration with tripolyphosphate cross-linked asymmetric chitosan membrane. J. Dentistry. 2014;42: 1603–1612. DOI: 10.1016/j.jdent.2014.08.015

[18] Uragami T, Saito T, Miyata T. Pervaporative dehydration characteristics of an ethanol/water azeotrope through various chitosan membranes. Carbohydrate Polymers. 2015;120: 1–6. DOI: 10.1016/j.carbpol.2014.11.032

[19] Alias S S, Ariff Z M, Mohamad A A. Porous membrane based on chitosan–SiO_2 for coin cell proton battery. Ceramics International. 2015;41: 5484–5491. DOI: 10.1016/j.ceramint.2014.12.119

[20] Puspasari T, Pradeep N, Peinemann K-V. Crosslinked cellulose thin film composite nanofiltration membranes with zero salt rejection. J. Membrane Science 2015;491: 132–137. DOI: 10.1016/j.memsci.2015.05.002

[21] Livazovic S, Li Z, Behzad A R, Peinemann K-V, Nunes S P. Cellulose multilayer membranes manufacture with ionic liquid. J. Membrane Science. 2015;490: 282–293. DOI: 10.1016/j.memsci.2015.05.009

[22] Zhang X, Lin B, Zhao K, Wei J, Guo J., Cui W, Jiang S, Liu D, Li J. A free-standing calcium alginate/polyacrylamide hydrogel nanofiltration membrane with high antifouling performance: Preparation and characterization. Desalination. 2015:365: 234–241. DOI: 10.1016/j.desal.2015.03.015

[23] Patel A K. Chitosan: Emergence as potent candidate for green adhesive market. Biochemical Engineering J..2015; 102: 74–81. DOI: 10.1016/j.bej.2015.01.005

[24] Bai H, Zhang H, He Y, Liu J, Zhang B, Wang J. Enhanced proton conduction of chitosan membrane enabled by halloysite nanotubes bearing sulfonate polyelectrolyte brushes. J. Membrane Science. 2014;454: 220–232. DOI: 10.1016/j.memsci.2013.12.005

[25] Tasselli F, Mirmohseni A, Seyed Dorraji M S, Figoli A. Mechanical, swelling and adsorptive properties of dry–wet spun chitosan hollow fibers crosslinked with glutaraldehyde. Reactive and Functional Polymers. 2013;73: 218–223. DOI: 10.1016/j.reactfunctpolym.2012.08.007

[26] Sun X, Wang Z, Kadouh H, Zhou K, The antimicrobial, mechanical, physical and structural properties of chitosan–gallic acid films. LWT - Food Science and Technology. 2014;57: 83–89. DOI: 10.1016/j.lwt.2013.11.037

[27] Wanichapichart P, Bootluck W, Thopan P, Yu L D. Influence of nitrogen ion implantation on filtration of fluoride and cadmium using polysulfone/chitosan blend membranes. Nuclear Instruments and Methods in Physics Research Section B: Beam Interactions with Materials and Atoms. 2014;326: 195–199. DOI: 10.1016/j.nimb.2013.10.091

[28] Shenvi S, Ismail A F, Isloor A M. Preparation and characterization study of PPEES/chitosan composite membrane crosslinked with tripolyphosphate. Desalination. 2014;344: 90–96. DOI: 10.1016/j.desal.2014.02.026

[29] Han F, Dong Y, Song A, Yin R, Li S. Alginate/chitosan based bi-layer composite membrane as potential sustained-release wound dressing containing ciprofloxacin hydrochloride. Applied Surface Science. 2014;311: 626–634. DOI: 10.1016/j.apsusc.2014.05.125

[30] Karim Z, Mathew A P, Grahn M, Mouzon J, Oksman K. Nanoporous membranes with cellulose nanocrystals as functional entity in chitosan: Removal of dyes from water. Carbohydrate Polymers. 2014;112: 668–676. DOI: 10.1016/j.carbpol.2014.06.048

[31] Dudek G, Gnus M, Turczyn R, Strzelewicz A, Krasowska M. Pervaporation with chitosan membranes containing iron oxide nanoparticles. Separation and Purification Technology. 2014;133: 8–15. DOI: 10.1016/j.seppur.2014.06.032

[32] Kumar R, Isloor A M, Ismail A F. Preparation and evaluation of heavy metal rejection properties of polysulfone/chitosan, polysulfone/N-succinyl chitosan and polysulfone/N-propylphosphonyl chitosan blend ultrafiltration membranes. Desalination. 2014;350: 102–108. DOI: 10.1016/j.desal.2014.07.010

[33] Sajjan A M, Premakshi H G, Kariduraganavar M Y. Synthesis and characterization of GTMAC grafted chitosan membranes for the dehydration of low water content isopropanol by pervaporation. J. Industrial and Engineering Chemistry. 2015;25: 151–161. DOI: 10.1016/j.jiec.2014.10.027

[34] Bibi S, Yasin T, Hassan S, Riaz M, Nawaz M. Chitosan/CNTs green nanocomposite membrane: Synthesis, swelling and polyaromatic hydrocarbons removal. Materials Science and Engineering C. 2015;46: 359–365. DOI: 10.1016/j.msec.2014.10.057

[35] Ji Y-L, An Q-F, Zhao F-Y, Gao C-J. Fabrication of chitosan/PDMCHEA blend positively charged membranes with improved mechanical properties and high nanofiltration performances. Desalination. 2015;357: 8–15. DOI: 10.1016/j.desal.2014.11.005

[36] Premakshi H G, Ramesh K, Kariduraganavar M Y. Modification of crosslinked chitosan membrane using NaY zeolite for pervaporation separation of water–isopropanol mixtures. Chemical Engineering Research and Design. 2015;94: 32–43. DOI: 10.1016/j.cherd.2014.11.014

[37] Santamaria M, Pecoraro C M, Quarto F D, Bocchetta P. Chitosan–phosphotungstic acid complex as membranes for low temperature H_2–O_2 fuel cell. J. Power Sources. 2015;276: 189–194. DOI: 10.1016/j.jpowsour.2014.11.147

[38] Zhu J, Tian M, Zhang Y, Zhang H, Liu J. Fabrication of a novel "loose" nanofiltration membrane by facile blending with Chitosan–Montmorillonite nanosheets for dyes purification. Chemical Engineering J.. 2015;265: 184–193. DOI: 10.1016/j.cej.2014.12.054

[39] Li Y-H, Cheng C-Y, Wang N-K, Tan H-Y, Tsai Y-J, Hsiao C-H, Ma D H-K, Yeh L-K. Characterization of the modified chitosan membrane cross-linked with genipin for the cultured corneal epithelial cells. Colloids and Surfaces B: Biointerfaces. 2015;126: 237–244. DOI: 10.1016/j.colsurfb.2014.12.029

[40] Hegab H M, Wimalasiri Y, Ginic-Markovic M, Zou L. Improving the fouling resistance of brackish water membranes via surface modification with graphene oxide functionalized chitosan. Desalination. 2015;365: 99–107. DOI: 10.1016/j.desal.2015.02.029

[41] Zhang D, Zhou W, Wei B, Wang X, Tang R, Nie J, Wang J. Carboxyl-modified poly (vinyl alcohol)-crosslinked chitosan hydrogel films for potential wound dressing. Carbohydrate Polymers. 2015;125: 189–199. DOI: 10.1016/j.carbpol.2015.02.034

[42] Panda S R, Mukherjee M, De S. Preparation, characterization and humic acid removal capacity of chitosan coated iron-oxide-polyacrylonitrile mixed matrix membrane. J. Water Process Engineering. 2015;6: 93–104. DOI: 10.1016/j.jwpe.2015.03.007

[43] Antunes B P, Moreira A F, Gaspar V M, Correia I J. Chitosan/arginine–chitosan polymer blends for assembly of nanofibrous membranes for wound regeneration. Carbohydrate Polymers. 2015;130: 104–112. DOI: 10.1016/j.carbpol.2015.04.072

[44] Song K, Gao A, Cheng X, Xie K. Preparation of the superhydrophobic nano-hybrid membrane containing carbon nanotube based on chitosan and its antibacterial activity. Carbohydrate Polymers. 2015;130: 381–387. DOI:10.1016/j.carbpol.2015.05.023

[45] Wang J, He R. Formation and evaluation of interpenetrating networks of anion exchange membranes based on quaternized chitosan and copolymer poly (acrylamide)/ polystyrene. Solid State Ionics. 2015;278: 49–57. DOI: 10.1016/j.ssi.2015.05.017

[46] Malini M, Thirumavalavan M, Yang W-Y, Lee J-F, Annadurai G. A versatile chitosan/ZnO nanocomposite with enhanced antimicrobial properties. International Journal of Biological Macromolecules. 2015;80: 121–129. DOI: 10.1016/j.ijbiomac. 2015.06.036

[47] Deuchi K, Kanauchi O, Imasato Y, Kobayashi E. Decreasing effect of chitosan on the apparent fat digestibility by rats fed on high-fat diet. Bioscience, Biotechnology, and biochemistry. 1994;58: 1613–1616. DOI: 10.1271/bbb.58.1613

[48] Yao H-T, Huang S-Y, Chiang M-T. A comparative study on hypoglycemic and hypocholesterolemic effects of high and low molecular weight chitosan in streptozotocin-induced diabetic rats. Food and Chemical Toxicology. 2008;46: 1525–1534. DOI: 10.1016/j.fct.2007.12.012

[49] Lu G, Kong L, Sheng B, Wang G, Gong Y, Zhang X. Degradation of covalently cross-linked carboxymethyl chitosan and its potential application for peripheral nerve regeneration. European Polymer J.. 2007;43: 3807–3818. DOI: 10.1016/j.eurpolymj. 2007.06.016

[50] Takahashi T, Imai M, Suzuki I. Water permeability of chitosan membrane involved in deacetylation degree control. Biochemical Engineering J.. 2007;36: 43–48. DOI: 10.1016/j.bej.2006.06.014

[51] Takahashi T, Imai M, Suzuki I. Cellular structure in an N-acetyl-chitosan membrane regulate water permeability. Biochemical Engineering J.. 2008;42: 20–27. DOI: 10.1016/j.bej.2008.05.013

[52] Santos C, Seabra P, Veleirinho B, Delgadillo I, Lopes da Silva J A. Acetylation and molecular mass effects on barrier and mechanical properties of shortfin squid chitosan membranes. European Polymer J.. 2006;42: 3277–3285. DOI: 10.1016/j.eurpolymj. 2006.09.001

[53] Ghosh A, Ali M A, Walls R. Modification of microstructural morphology and physical performance of chitosan films. International J. Biological Macromolecules. 2010;46: 179–186. DOI: 10.1016/j.ijbiomac.2009.11.006

[54] Jin J, Song M, Hourston D J. Novel chitosan-based films cross-linked by genipin with improved physical properties. Biomacromolecules. 2004;5: 162–168. DOI: 10.1021/ bm034286m

[55] Remuñán-López C, Bodmeier R. Mechanical, water uptake and permeability properties of crosslinked chitosan glutamate and alginate films. J. Controlled Release. 1997;44: 215–225. DOI: 10.1016/S0168-3659 (96)01525-8

[56] Lee Y M, Nam S Y, Woo D J. Pervaporation of ionically surface crosslinked chitosan composite membranes for water-alcohol mixtures. J. Membrane Science. 1997;133: 103–110. DOI: 10.1016/S0376-7388 (97)00089-6

[57] Devi D A, Smitha B, Sridhar S, Aminabhavi T M. Pervaporation separation of isopropanol/water mixtures through crosslinked chitosan membranes. J. Membrane Science. 2005;262: 91–99. DOI: 10.1016/j.memsci.2005.03.051

[58] Cottrell I W, Kovacs P. Alginate. In: Davidson R L, editor.Handbook of water-soluble gums and resins. New York: McGraw-HillInc.;1980. P. 2-1–2-43.

[59] Baffoun A, Viallier P, Dupuis D, Haidara H. Drying morphologies and related wetting and impregnation behaviours of 'sodium-alginate/urea' inkjet printing thickeners. Carbohydrate Polymers. 2005; 61: 103–110. DOI: 10.1016/j.carbpol.2005.03.018

[60] Richardson J C, Dettmar P W, Hampson F C, Melia C D. Oesophageal bioadhesion of sodium alginate suspensions: 2. Suspension behaviour on oesophageal mucosa.European J. Pharmaceutical Sciences. 2005; 24: 107–114. DOI: 10.1016/j.ejps.2004.10.001

[61] Rescignano N, Fortunati E, Armentano I, Hernandez R, Mijangos C, Pasquino R, Kenny J M. Use of alginate, chitosan and cellulose nanocrystals as emulsion stabilizers in the synthesis of biodegradable polymeric nanoparticles. J. Colloid Interface Science. 2015; 445: 31–39. DOI: 10.1016/j.jcis.2014.12.032

[62] Yang Y, Campanella O H, Hamaker B R, Zhang G, Gu Z. Rheological investigation of alginate chain interactions induced by concentrating calcium cations. Food Hydrocolloids. 2013; 30: 26–32. DOI: 10.1016/j.foodhyd.2012.04.006

[63] Li J, He J, Huang Y, Li D, Chen X. Improving surface and mechanical properties of alginate films by using ethanol as a co-solvent during external gelation. Carbohydrate Polymers. 2015; 123: 208–216. DOI: 10.1016/j.carbpol.2015.01.040

[64] Ha T L B, Quan T M, Vu D N, Si D M. Naturally Derived Biomaterials: Preparation and Application. In: Andrades J A, editor. Regenerative Medicine and Tissue Engineering. Croatia: InTech; 2013. p. 247–274. DOI: 10.5772/55668

[65] Kashima K, Imai M. Impact factors to regulate mass transfer characteristics of stable alginate membrane performed superior sensitivity on various organic chemicals. Procedia Engineering. 2012; 42: 964–977. DOI: 10.1016/j.proeng.2012.07.490

[66] Toti U S, Aminabhavi T M. Different viscosity grade sodium alginate and modified sodium alginate membranes in pervaporation separation of water + acetic acid and water + isopropanol mixtures. J. Membrane Science. 2004;228: 199–208. DOI: 10.1016/j.memsci.2003.10.008

[67] Kalyani S, Smitha B, Sridhar S, Krishnaiah A. Pervaporation separation of ethanol–water mixtures through sodium alginate membranes. Desalination. 2008;229: 68–81. DOI: 10.1016/j.desal.2007.07.027

[68] Saraswathi M, Madhusudhan Rao K, Prabhakar M N, Prasad C V, Sudakar K, Naveen Kumar H M P, Prasad M, Chowdoji Rao K, Subha M C S. Pervaporation studies of sodium alginate (SA)/dextrin blend membranes for separation of water and isopropanol mixture. Desalination. 2011;269: 177–183. DOI: 10.1016/j.desal.2010.10.059

[69] Li Y, Jia H, Cheng Q, Pan F, Jiang Z. Sodium alginate–gelatin polyelectrolyte complex membranes with both high water vapor permeance and high permselectivity. J. Membrane Science. 2011;375: 304–312. DOI: 10.1016/j.memsci.2011.03.058

[70] Taşkın G, Şanlı O, Asman G. Swelling assisted photografting of itaconic acid onto sodium alginate membranes. Applied Surface Science. 2011;257: 9444–9450. DOI: 10.1016/j.apsusc.2011.06.030

[71] Chen J H, Liu Q L, Hu S R, Ni J C, He Y S. Adsorption mechanism of Cu (II) ions from aqueous solution by glutaraldehyde crosslinked humic acid-immobilized sodium alginate porous membrane adsorbent. Chemical Engineering J.. 2011;173: 511–519. DOI: 10.1016/j.cej.2011.08.023

[72] Li Y, Jia H, Pan F, Jiang Z, Cheng Q. Enhanced anti-swelling property and dehumidification performance by sodium alginate–poly (vinyl alcohol)/polysulfone composite hollow fiber membranes. J. Membrane Science. 2012;407–408: 211–220. DOI: 10.1016/j.memsci.2012.03.049

[73] Nigiz F U, Dogan H, Hilmioglu N D. Pervaporation of ethanol/water mixtures using clinoptilolite and 4A filled sodium alginate membranes. Desalination. 2012;300: 24–31. DOI: 10.1016/j.desal.2012.05.036

[74] Sajjan A M, Jeevan Kumar B K, Kittur A A, Kariduraganavar M Y. Novel approach for the development of pervaporation membranes using sodium alginate and chitosan-wrapped multiwalled carbon nanotubes for the dehydration of isopropanol. J. Membrane Science. 2013;425–426: 77–88. DOI: 10.1016/j.memsci.2012.08.042

[75] Flynn E J, Keane D, Holmes J D, Morris M A. Unusual trend of increasing selectivity and decreasing flux with decreasing thickness in pervaporation separation of ethanol/water mixtures using sodium alginate blend membranes. J. Colloid and Interface Science. 2012;370: 176–182. DOI: 10.1016/j.jcis.2011.12.022

[76] Shi J, Shi J, Du C, Chen Q, Cao S. Thermal and pH dual responsive alginate/$CaCO_3$ hybrid membrane prepared under compressed CO_2. J. Membrane Science. 2013;433: 39–48. DOI: 10.1016/j.memsci.2013.01.021

[77] Chen J H, Xing H T, Guo H X, Li G P, Weng W, Hu S R. Preparation, characterization and adsorption properties of a novel 3-aminopropyltriethoxysilane functionalized sodium alginate porous membrane adsorbent for Cr (III) ions. J. Hazardous Materials. 2013;248–249: 285–294. DOI: 10.1016/j.jhazmat.2013.01.042

[78] Zhu Y, Wang Z, Zhang C, Wang J, Wang S. A novel membrane prepared from sodium alginate cross-linked with sodium tartrate for CO_2 capture. Chinese J. Chemical Engineering. 2013;21: 1098–1105. DOI: 10.1016/S1004-9541 (13)60574-1

[79] Adoor S G, Rajineekanth V, Nadagouda M N, Rao K C, Dionysiou D D, Aminabhavi T M. Exploration of nanocomposite membranes composed of phosphotungstic acid in sodium alginate for separation of aqueous–organic mixtures by pervaporation. Separation and Purification Technology. 2013;113: 64–74. DOI: 10.1016/j.seppur.2013.03.051

[80] Zhang W, Xu Y, Yu Z, Lu S, Wang X. Separation of acetic acid/water mixtures by pervaporation with composite membranes of sodium alginate active layer and microporous polypropylene substrate. J. Membrane Science. 2014;451: 135–147. DOI: 10.1016/j.memsci.2013.09.027

[81] Gao C, Zhang M, Ding J, Pan F, Jiang Z, Li Y, Zhao J. Pervaporation dehydration of ethanol by hyaluronic acid/sodium alginate two-active-layer composite membranes. Carbohydrate Polymers. 2014;99: 158–165. DOI: 10.1016/j.carbpol.2013.08.057

[82] Kuila S B, Ray S K. Dehydration of dioxane by pervaporation using filled blend membranes of polyvinyl alcohol and sodium alginate. Carbohydrate Polymers. 2014;101: 1154–1165. DOI: 10.1016/j.carbpol.2013.09.086

[83] Kuila S B, Ray S K. Separation of benzene–cyclohexane mixtures by filled blend membranes of carboxymethyl cellulose and sodium alginate. Separation and Purification Technology. 2014;123: 45–52. DOI: 10.1016/j.seppur.2013.12.017

[84] Yang J-M, Wang N-C, Chiu H-C. Preparation and characterization of poly (vinyl alcohol)/sodium alginate blended membrane for alkaline solid polymer electrolytes membrane. J. Membrane Science. 2014;457: 139–148. DOI: 10.1016/j.memsci.2014.01.034

[85] Pasini Cabello S D, Mollá S, Ochoa N A, Marchese J, Giménez E, Compañ V. New bio-polymeric membranes composed of alginate-carrageenan to be applied as polymer electrolyte membranes for DMFC. J. Power Sources. 2014;265: 345–355. DOI: 10.1016/j.jpowsour.2014.04.093

[86] Cao K, Jiang Z, Zhao J, Zhao C, Gao C, Pan F, Wang B, Cao X, Yang J. Enhanced water permeation through sodium alginate membranes by incorporating graphene oxides. J. Membrane Science. 2014;469: 272–283. DOI: 10.1016/j.memsci.2014.06.053

[87] Yoo S M, Ghosh R. Fabrication of alginate fibers using a microporous membrane based molding technique. Biochemical Engineering J.. 2014;91: 58–65. DOI: 10.1016/j.bej.2014.07.006

[88] Kamoun E A, Kenawy E-R S, Tamer T M, El-Meligy M A, Eldin M S M. Poly (vinyl alcohol)-alginate physically crosslinked hydrogel membranes for wound dressing

applications: Characterization and bio-evaluation. Arabian J. Chemistry. 2015;8: 38–47. DOI: 10.1016/j.arabjc.2013.12.003

[89] Li J, He J, Huang Y, Li D, Chen X. Improving surface and mechanical properties of alginate films by using ethanol as a co-solvent during external gelation. Carbohydrate Polymers. 2015;123: 208–216. DOI: 10.1016/j.carbpol.2015.01.040

[90] Soazo M, Báez G, Barboza A, Busti P A, Rubiolo A, Verdini R, Delorenzi N J. Heat treatment of calcium alginate films obtained by ultrasonic atomizing: Physicochemical characterization. Food Hydrocolloids. 2015;51: 193–199. DOI: 10.1016/j.foodhyd.2015.04.037

[91] Zhao K, Zhang X, Wei J, Li J, Zhou X, Liu D, Liu Z, Li J. Calcium alginate hydrogel filtration membrane with excellent anti-fouling property and controlled separation performance. J. Membrane Science. 2015;492: 536–546. DOI: 10.1016/j.memsci.2015.05.075

[92] Jie G, Kongyin Z, Xinxin Z, Zhijiang C, Min C, Tian C, Junfu W. Preparation and characterization of carboxyl multi-walled carbon nanotubes/calcium alginate composite hydrogel nano-filtration membrane. Materials Letters. 2015;157: 112–115. DOI: 10.1016/j.matlet.2015.05.080

[93] Kirdponpattara S, Khamkeaw A, Sanchavanakit N, Pavasant P, Phisalaphong M. Structural modification and characterization of bacterial cellulose–alginate composite scaffolds for tissue engineering. Carbohydrate Polymers. 2015;132: 146–155. DOI: 10.1016/j.carbpol.2015.06.059

[94] Shao W, Liu H, Liu X, Wang S, Wu J, Zhang R, Min H, Huang M. Development of silver sulfadiazine loaded bacterial cellulose/sodium alginate composite films with enhanced antibacterial property. Carbohydrate Polymers. 2015;132: 351–358. DOI: 10.1016/j.carbpol.2015.06.057

[95] Uragami T, Banno M, Miyata T. Dehydration of an ethanol/water azeotrope through alginate-DNA membranes cross-linked with metal ions by pervaporation. Carbohydrate Polymers. 2015;134: 38–45. DOI: 10.1016/j.carbpol.2015.07.054

[96] Haug A, Larsen B, Smidsrød O. A study of the constitution of alginic acid by partial acid hydrolysis. Acta Chemica Scandinavica. 1966;20: 183–190. DOI: 10.3891/acta.chem.scand.20-0183

[97] Haug A, Larsen B, Smidsrød O. Uronic acid sequence in alginate from different sources. Carbohydrate Research. 1974;32: 217–225. DOI: 10.1016/S0008-6215 (00)82100-X

[98] Gacesa P. Alginates. Carbohydr. Polym. 1988;8: 161–182. DOI: 10.1016/0144-8617 (88)90001-X

[99] Draget K I, Smidsrød O, Skjåk-Bræk G. Alginates from algae. In: Steinbuchel A, Rhee S K, editors. Polysaccharides and Polyamides in the Food Industry, Properties, Pro-

duction and Patents. Weinheim: Wiley–VCH; 2005. P. 1-30. DOI: 10.1002/3527600035.bpol6008

[100] Grant G T, Morris E R, Rees D A, Smith P J C, Thom D. Biological interactions between polysaccharides and divalent cations: The egg-box model. FEBS Letters. 1973;32: 195–198. DOI: 10.1016/0014-5793 (73)80770-7

[101] Kashima K, Imai M. Advanced membrane material from marine biological polymer and sensitive molecular-size recognition for promising separation technology. In: Ning R Y, editor. Advancing Desalination. Croatia: InTech; 2012. p. 3–36. DOI: 10.5772/50734

[102] Bitter T, Muir H M. A modified uronic acid carbazole reaction. Analytical Biochemistry. 1962;4: 330–334. DOI: 10.1016/0003-2697 (62)90095-7

[103] Anzai H, Uchida N, Nishide E. Determination of D-mannuronic to L-guluronic acids ratio in acid hydrolysis of alginate under improved conditions. Nippon Suisan Gakkaishi. 1990;56: 73–81. DOI: 10.2331/suisan.56.73

[104] Anzai H, Uchida N, Nishide E. Comparative studies of colorimetric analysis for uronic acids. Bulletin of the College of Agriculture and Veterinary Medicine Nihon University. 1986;43: 53–56 (in Japanese).

[105] Wilke C R, Chang P. Correlation of diffusion coefficients in dilute solutions. A. I. Ch. E. J. 1955;1: 264–270. DOI: 10.1002/aic.690010222

[106] Smidsrød O. Molecular basis for some physical properties of alginates in the gel state. Faraday Discussions of the Chemical Society.1974; 57: 263–274. DOI: 10.1039/DC9745700263

[107] Donati I, Paoletti S. Material Properties of Alginates, In: B H. A. Rehm editor, Alginates: Biology and Applications. Berlin: Springer; 2009. p. 1–53. DOI: 10.1007/978-3-540-92679-5_1

[108] So M T, Eirich F R, Strathmann H, Baker R W. Preparation of Asymmetric Loeb-Sourirajan Membranes. J. Polymer Science: Polymer Letters Edition. 1973;11: 201–205. DOI: 10.1002/pol.1973.130110311